Eastern Region Technical Attachment
No. 2020-03
February 2020

Using Multi-Radar Multi-Sensor (MRMS) Vertically Integrated Ice (VII) to assess cloud-to-ground lightning initiation potential for use in IDSS

*Corey Bogel and Francis Kredensor**
NOAA/National Weather Service
Caribou, Maine

Abstract

The intent of this study is to investigate the use of multi-radar/multi-sensor (MRMS) vertically integrated ice (VII) as a lightning nowcasting tool, with the goal of providing forecasters with greater confidence and skill in assessing the potential for cloud-to-ground (CG) lightning strikes. This may aid forecasters in impact-based decision support services (IDSS) as it relates to CG lightning initiation. The use of MRMS VII may be useful for identifying storm initiation and the onset of electrical activity. Prior to MRMS, VII was not available operationally, but now VII can be used as a lightning nowcasting tool. VII is derived from a 3D reflectivity cube by vertically integrating reflectivity from -10 °C to -40 °C using the Rapid Refresh (RAP) model and converting to mass/area. Several hundred lightning and non-lightning producing cells were examined across the National Weather Service (NWS) Caribou, Maine area of forecast responsibility. The probability of detection (POD), critical success index (CSI), and false alarm rate (FAR) were calculated for various isothermal reflectivity levels and VII thresholds. This study showed that the greatest lead time to CG lightning initiation was associated with the lowest values of VII, which at the time of the study was 1.0 kg m^{-2}.

**Current Affiliation and corresponding author address: Francis Kredensor, NOAA/National Weather Service, 5324 Tri-Hill Frontage Road, Great Falls, MT 59404.*
E-mail: Francis.Kredensor@noaa.gov

1. Introduction

Cloud-to-ground lightning is responsible for a 30-year average of 48 fatalities annually in the United States. Maps of U.S. lightning deaths from 2008-2017 (Fig.1) shows that Maine ranked between 11th and 20th for lightning fatalities weighted by population from 2008-2017 (Fig.2). Based on media reports of the fatal incidents, many victims were either headed to safety at the time of the fatal strike or were just steps away from safety. Continued efforts are needed to convince people to get inside a safe place before the lightning threat becomes significant. For many activities, situational awareness and proper planning are essential to safety (Jensenius 2019). Leisure activities contributed to 62% of the overall deaths from lightning, and water related activities were the largest contributor among leisure-related fatalities (Fig.3). Water-related activities such as fishing, boating, swimming, or just relaxing at a beach or lake are common outdoor activities in Maine during the summer. Factors that contribute to lightning fatalities include: Unwillingness to cancel or postpone activities, being unaware of approaching or developing storms, vulnerability of the activity, and the inability and unwillingness to get to a safe place quickly (Jensenius 2019).

Improved lead time and forecaster confidence in the initiation of CG lightning could significantly improve IDSS and public safety. Once CG lighting has been detected, it can be relatively easy to track. However, the first CG strike can be particularly hazardous if it develops overhead or nearby. Therefore, it can be of great benefit for IDSS to anticipate the first CG strike. Holle et al. (1992) determined that most casualties from lightning occur either when the leading edge of a storm first approaches the victim, or when the back end of a storm is leaving the victim's location. At these times the public may not be fully aware of the threat of lightning. Therefore, forecasting lightning initiation and cessation within thunderstorms is vital in protecting lives (Seroka, et al. 2012).

Currently, one of the most common methods forecasters use to predict lightning initiation is to observe when developing cells reach certain reflectivity thresholds at specific isothermal levels associated with ice formation in the cloud. In their literature review, Mosier et al. (2011) determined that having a cell reach 40 dBZ reflectivity at the -10 °C isothermal level tended to produce the best lightning forecasts in previous studies (Buechler and Goodman 1990; Gremillion and Orville 1999; Wolf 2007) as measured by CSI. However, this method requires forecasters to assess the current isothermal levels from soundings that may be hours old and/or hundreds of miles away, and they must interpolate between radar elevation scans if no one scan passes through a cell close to their desired isothermal level. MRMS helps ameliorate these limitations by using hourly RAP model analyses to assess isothermal level heights across the area. MRMS then combines the RAP data with mosaics of multiple radars to produce intuitive isothermal reflectivity products that require no mental gymnastics on the part of the forecaster (Smith et al. 2016).

This study is meant to extend the work of Mosier et al. (2011) and Seroka et al. (2012) to an area across the northern contiguous United States. Those studies used the reflectivity-ice mass equation from Carey

and Rutledge (2000) to calculate vertically integrated ice (VII) data from archived single-site radar data, as prior to MRMS, VII data was not available operationally. Email correspondence with Mosier and the Science and Operations Officer at WFO Fort Worth/Dallas (FWD) revealed that an attempt was made to get real-time VII data available to forecasters at FWD, but there were latency and system resource issues that impacted its operational usefulness (Moisier, personal communication, 2017 and Ryan, personal communication, 2017). We seek to extend their work now that VII analyses are available for real-time operations via the MRMS suite of products. This study attempts to explore the potential for utilizing MRMS isothermal reflectivity and VII data to develop an experimental CG lightning risk map, perhaps using risk level categories. Such a tool could provide decision makers with a valuable resource to assess the near-term lightning risk in a time scale of less than 1 hour.

The following sections of this paper will examine the data and methodology used, discuss the findings, make recommendations, and highlight areas worthy of future investigation.

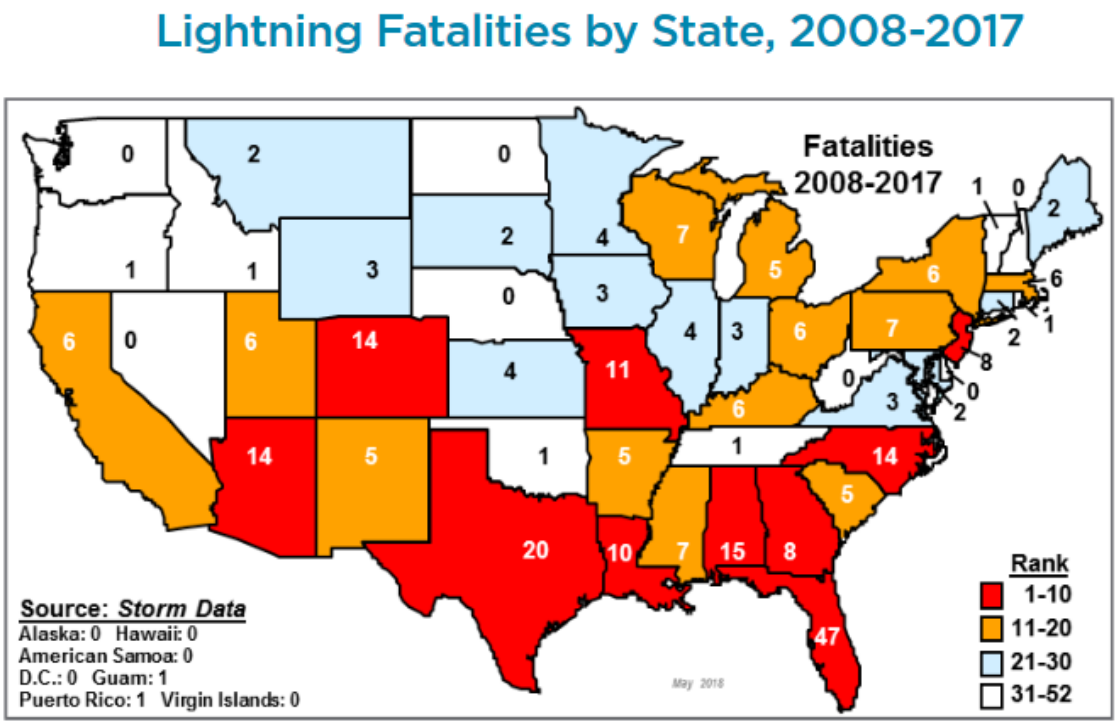

Figure 1. Lightning fatalities in the U.S. by state from 2008-2017. Figure from Ron Holle (Vaisala Inc.) and available at the NWS's www.weather.gov/safety/lightning web site.

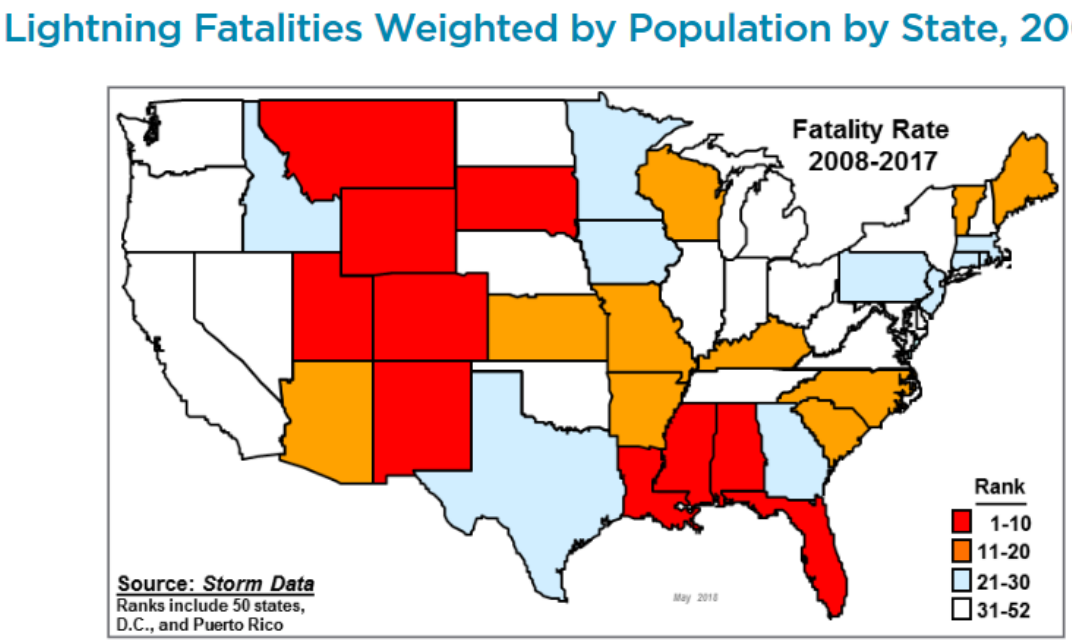

Figure 2. Lightning fatalities weighted by population by state, 2008-2017. Figure from Ron Holle (Vaisala Inc.) and available at the NWS's www.weather.gov/safety/lightning web site.

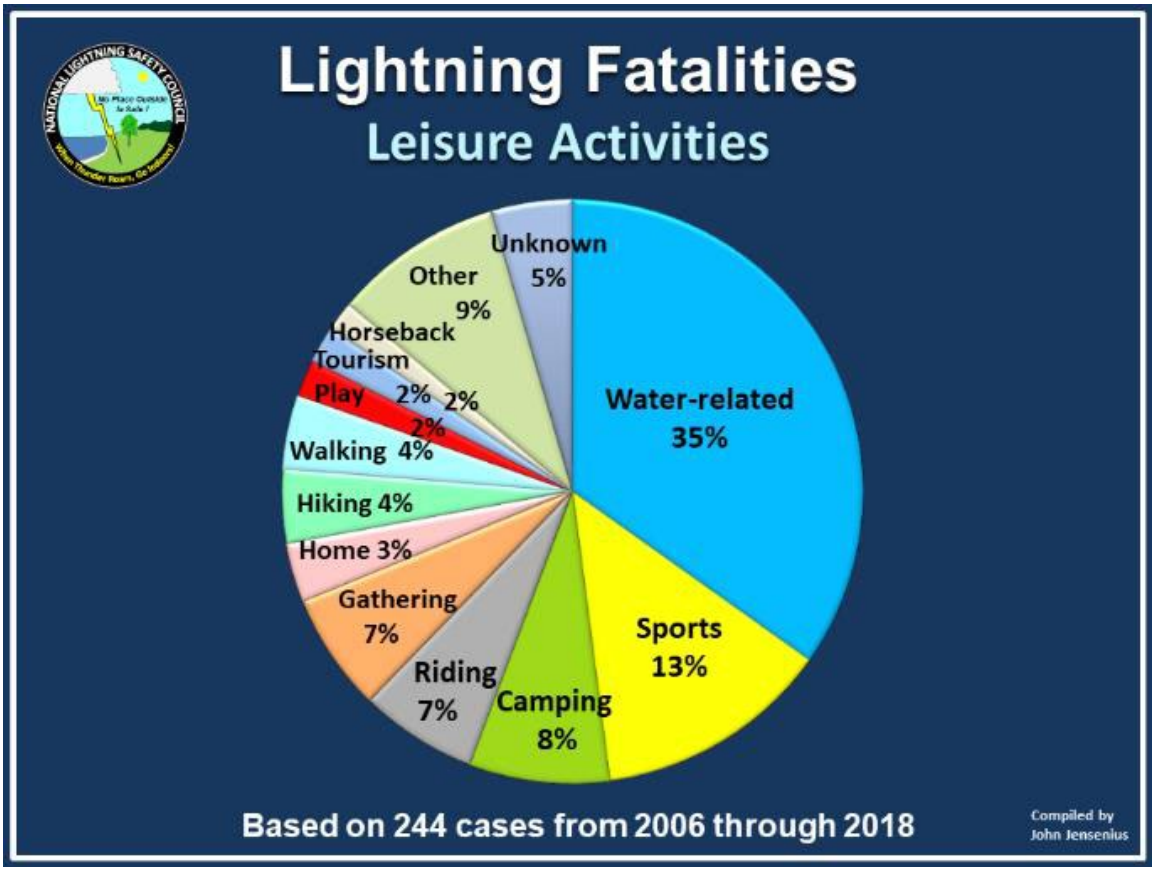

Figure 3. Percent of deaths by sub-category for leisure activities. Figure from Jensenius (2019).

2. Data and Methodology

Convective cells were collected from numerous days in August and September 2017 with convection across the Caribou, Maine, County Warning Area (CWA) and adjoining portions of New Brunswick (Fig. 4). Prospective cells were identified using ID tags from the Storm Cell Identification and Tracking (SCIT) algorithm (Johnson, et al. 1998), as displayed in the AWIPS Storm Track Information (STI) product. Both lightning and non-lightning producing convective cells were manually tracked. National Lightning Detection Network (NLDN) data was used to determine if a CG lightning strike occurred in association with a cell. It is important to note that lightning that occurred in stratiform precipitation areas was not utilized for this study. Out of 392 cells tracked and analyzed for this study, 170 cells (43.4%) produced CG lightning strikes. The efficacy of various MRMS isothermal reflectivity and MRMS VII thresholds was measured by calculating the Probability of Detection (POD), False Alarm Rate (FAR), and Critical Success Index (CSI) for each threshold tracked. The lead time for the first CG lightning strike was also computed for the various reflectivity levels and VII values. Statistics computed for the lightning and null cases help inform a framework for improved nowcasting of lightning to provide as much lead time as possible.

The study was somewhat subjective in nature with manual tracking of cells, unlike previous research by Mosier et al. (2011) and Seroka et al. (2012), in which cells were objectively analyzed and automatically tracked using a modified version of the SCIT algorithm and lightning strikes were automatically assigned to a cell for the areas around Houston, Texas, and Melbourne, Florida, respectively. To allow easy review of cells in this study, only those cells assigned an ID tag by the STI product were considered for inclusion in this study. Additional constraints, as detailed below, were also used. Lightning strikes were manually reviewed and assigned to cells, and this method is described below.

We assigned the additional condition that there had to be an appreciable contiguous area (at least ten 1 km^2 pixels) of 40 dBZ or higher returns for at least 6 time steps (10 minutes) of the MRMS Reflectivity at Lowest Altitude (RALA) data (products are produced every 2 minutes). This was the most subjective part of the analysis. The STI product would often lag in assigning an ID tag on a cell that already appeared to be robust, and data was collected on cells prior to the STI ID being assigned, provided it had the aforementioned area of 40 dBZ or greater returns on the MRMS RALA product. This was done to account for how a human radar operator might ID and track cells worth watching faster than the algorithm. The STI product occasionally had problems with cell identification and tracking, and the following modifications were allowed. Cells identified by the STI algorithm in areas of stratiform precipitation were not included, unless a cell with clearly defined boundaries and higher reflectivity moved into or through a stratiform area with lower reflectivity. If the STI algorithm gave one cell multiple ID tags through the cell's lifecycle, it was treated as one continuous cell and the multiple ID tags were all included in the database entry for that cell. Finally, if the STI ID tag jumped from one cell to another nearby cell, both cells could be included in the study provided they both met all other above qualifications.

For the assignment of lightning strikes to cells, the following methodology was used. CG lightning strikes clearly occurring within the boundaries of a distinct cell, as defined by a contiguous 40dBZ or greater area on the MRMS RALA product, were assigned to that cell. If a CG lightning strike occurred away from any one cell, it was assigned to the closest cell. Lightning strikes occurring in stratiform precipitation areas were ignored. Only the first CG lightning strike associated with a cell was recorded. Once a cell's first CG strike was identified (if it produced a CG strike), researchers calculated lead times for various isothermal reflectivity and VII thresholds by noting how far in advance a cell first attained those thresholds, and noting which thresholds (if any) were not met. For the purposes of POD calculation, a 'correct forecast' is where a cell achieved a particular threshold at or before the time of the first CG strike. A 'missed event' is defined as where a cell met that threshold after the first CG strike was recorded, or where the cell did not achieve the threshold at all during its lifecycle. A 'false alarm' is an instance where a cell reached a particular threshold, but the cell never produced a CG strike.

The average lead time, CSI, FAR, and POD for MRMS isothermal reflectivity thresholds at 25, 30, 35, and 40 dBZ at -10°C and -20°C were examined. These statistics were also computed for the MRMS VII values from 1 to 10 kg m^{-2} at 0.5 kg m^{-2} intervals.

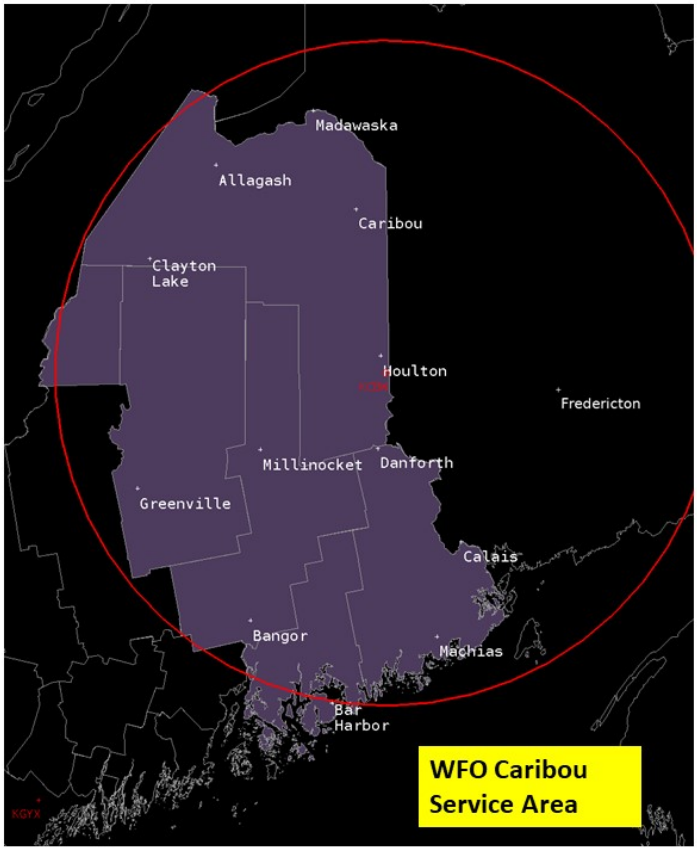

Figure 4. Caribou, Maine CWA with a 100 NM range ring around the Hodgdon, Maine (KCBW) WSR-88Dweather radar.

3. Results and Discussion

A total of 170 cells examined as part of this study produced CG lightning. Lead time in this paper is defined as the time elapsed from the first time a cell reached a particular reflectivity or VII threshold to the first NLDN CG strike. For MRMS isothermal reflectivity, the greatest average lead time of 25.3 minutes was observed at the -10°C isotherm at the 25 dBZ reflectivity threshold. The lead time diminished with increasing reflectivity thresholds (Fig.5). This was the case at both the -10°C and -20 °C isotherms. These trends were expected, as lower reflectivity thresholds will be reached earlier, and warmer (lower altitude) isothermal levels will be attained before colder levels.

The lead time was also examined for VII Thresholds (Fig.6) with the greatest average lead time of 19.2 minutes to CG strikes noted at 1.0 kg m^{-2}, rapidly diminishing to a lead time of around 10 minutes from 3.0 kg m^{-2} to 6.5 kg m^{-2} . A further degradation of lead time was observed with VII values from 7 kg m^{-2} to 8.5 kg m^{-2}. The slight increase in lead time seen at the highest values of VII may be an artifact owing to the small sample size of cells that attained those VII thresholds.

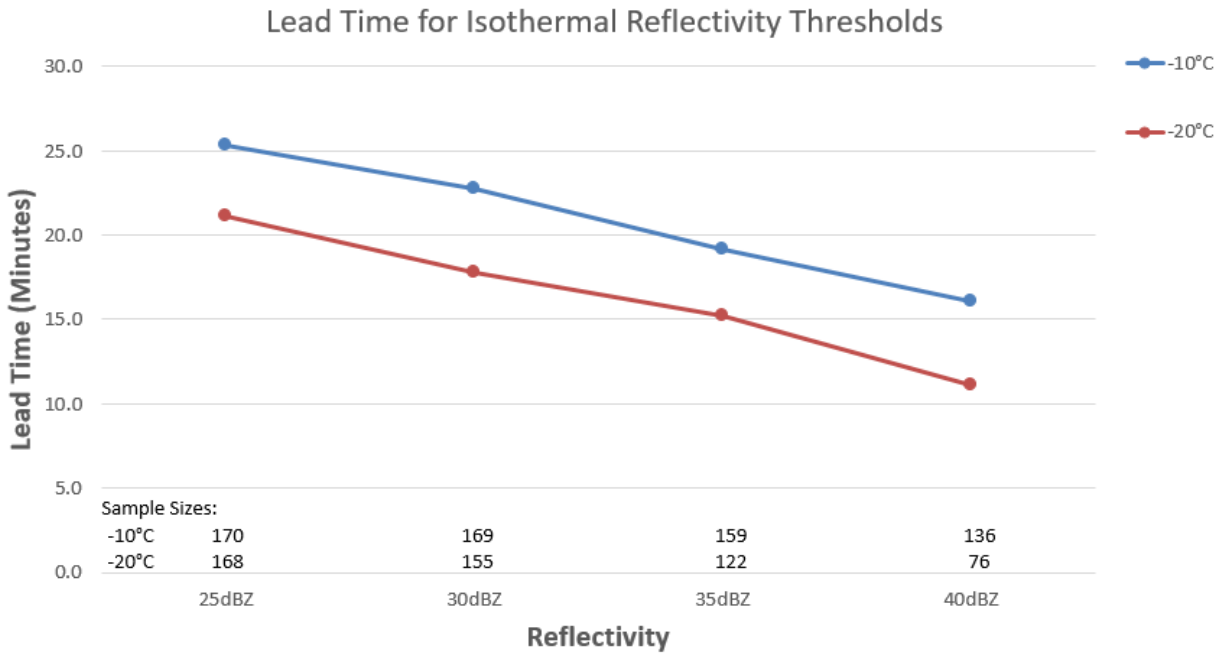

Figure 5. Lead time (min) for isothermal reflectivity thresholds. The sample size noted for each threshold is the total number of correct lightning forecasts at each threshold.

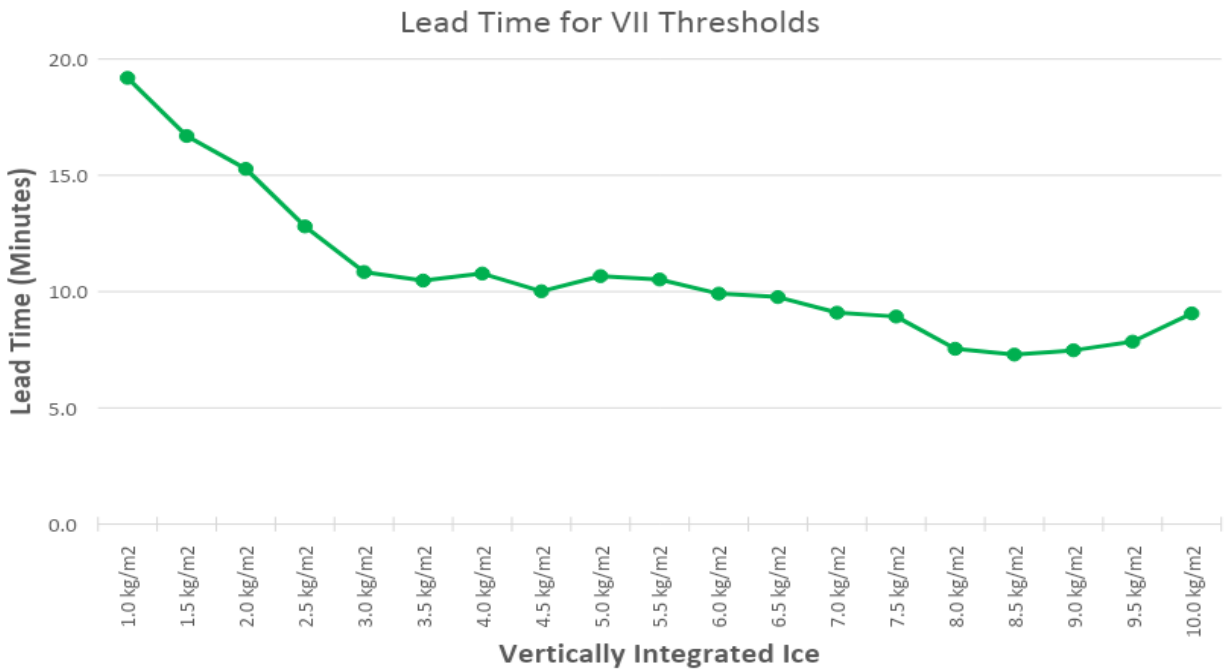

Figure 6. Same as Fig. 5, but for VII thresholds.

The POD, FAR, and CSI were examined for isothermal reflectivity thresholds (Figs. 7-9). Statistics were calculated based on thresholds being reached prior to the first CG strike (a hit), while a miss equated to the first strike occurring prior to the reflectivity threshold being reached. The POD was 1.00 for the 25 dBZ value at the -10 °C isothermal level, and dropped to a low of 0.45 for the 40 dBZ value at the -20°C isothermal level. The highest FAR of 0.56 was associated with the 25 dBZ value at -10 °C with steadily lower FAR values noted at the 30, 35, and 40 dBZ values of both the -10 and -20 °C isothermal levels. The lowest FAR of 0.35 was observed with the 40 dBZ value at the -20 °C level. Of course, it is likely that some of the false alarm cells did produce in-cloud lightning, but not cloud-to-ground lightning, as Seroka et al (2012) found that approximately 30% of lightning-producing cells in that study produced only in-cloud lightning.

The CSI values at the -10 °C isothermal level varied little from 0.43-0.47 based on the 25, 30, 35, and 40 dBZ values that were examined. At the -20 °C isothermal level, the CSI ranged from 0.45-0.48 at the 25, 30, and 35 dBZ values, but dropped to 0.36 at the 40 dBZ level. In general, the results for POD and FAR are what should be expected, with both having higher values at lower reflectivity thresholds, and decreasing at higher reflectivity. From previous studies assessed by Mosier et al. (2012), the 40 dBZ threshold at -10 °C was expected to perform well, and it indeed did have the second highest CSI score at 0.47. However, the 30 dBZ reflectivity threshold at -20 °C performed equally well with a CSI of 0.48, indicating its usefulness as a CG lightning predictor. Many of the other reflectivity thresholds also scored highly, with CSI values close to these top performers, indicating that the best threshold to use in a given situation may depend on whether maximizing POD or minimizing FAR is more important.

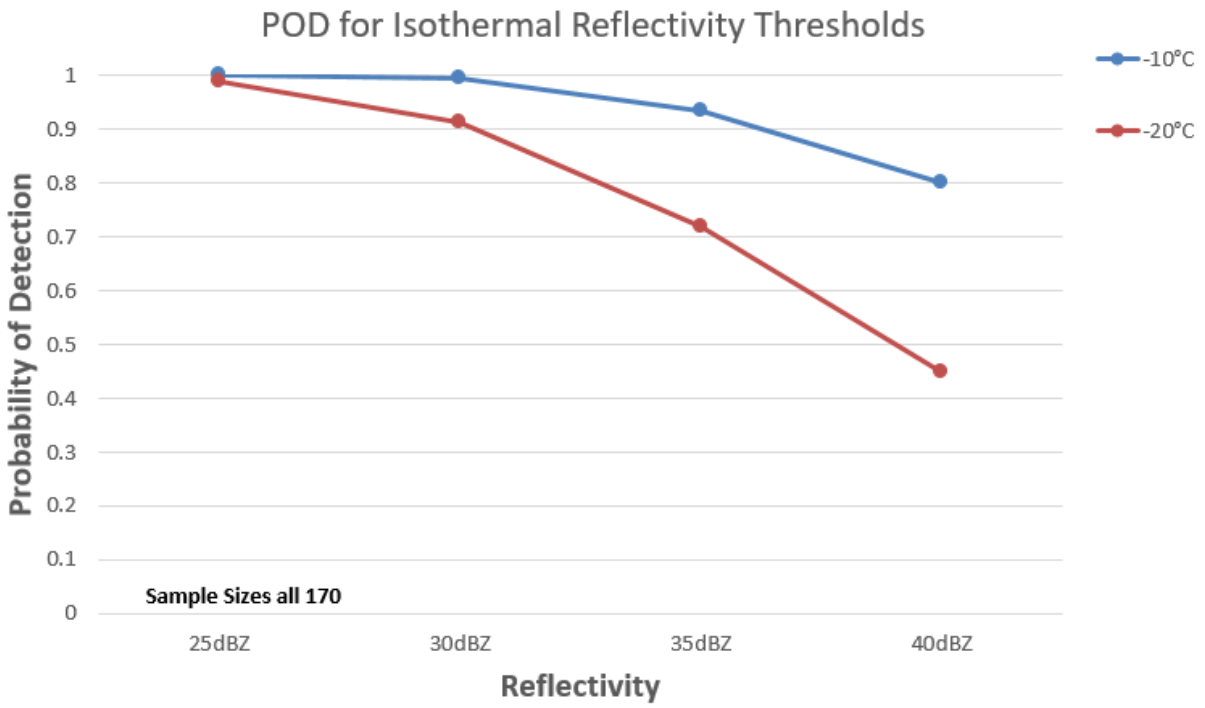

Figure 7. The POD for the 25, 30, 35, and 40 dBZ isothermal reflectivity thresholds. The sample size for all thresholds is 170, which is the total number of cells that produced lightning.

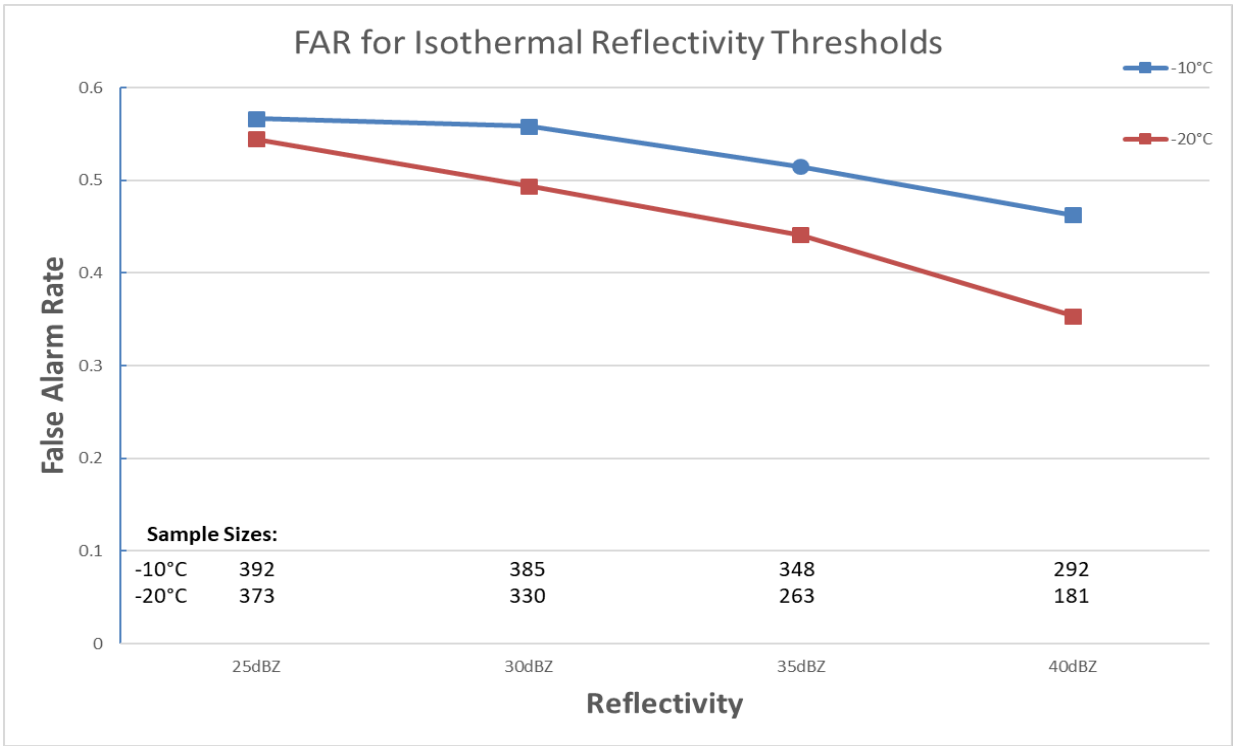

Figure 8. The FAR for the 25, 30, 35, and 40 dBZ isothermal reflectivity thresholds. The sample size noted for each threshold is the total number of cells (whether correct, false alarm, missed event) observed at each threshold.

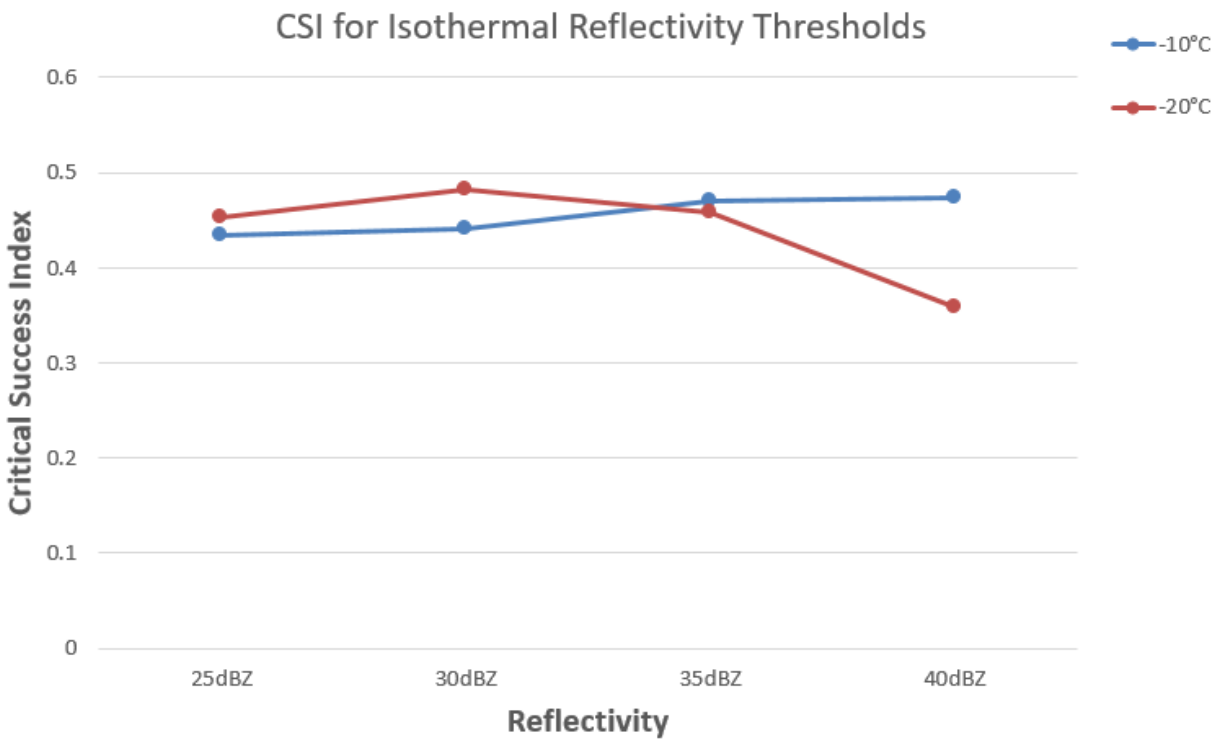

Figure 9. The CSI for the 25, 30, 35 and 40 dBZ isothermal reflectivity thresholds.

The POD, FAR, and CSI were examined for the VII thresholds (Figs. 10-12) from 1 to 10 kg m^{-2}. The POD was 0.93 for a VII of 1 kg m^{-2} and dropped off to less than 0.5 at a VII of 3.5, and to less than 0.2 at values greater than 6.5 kg m^{-2}. The FAR was just over 0.5 at a VII value of 1.0 kg m^{-2} and steadily decreased with increasing VII values. The lowest FAR of just 0.1 was observed with VII values of 10 kg m^{-2}. Like with the isothermal reflectivity thresholds, some of the VII false alarm cells could have produced in-cloud lightning but not CG lightning. The CSI followed the same general trend as the FAR with the greatest CSI observed with the lowest VII values. The peak CSI values are lower than for similar values of VII in the Mosier et al. (2011) study and similar to the findings of the Seroka et al. (2012) study, the trends match up with what was expected based on both of those earlier works.

It is important to note that the highest CSI values for VII of 0.48, found at VII values of 1.0 kg m^{-2} to 2.0 kg m^{-2}, were almost identical to the highest CSI values for MRMS isothermal reflectivity of 0.47-0.48. This points to MRMS VII being comparable to isothermal reflectivity in usefulness for predicting CG lightning initiation.

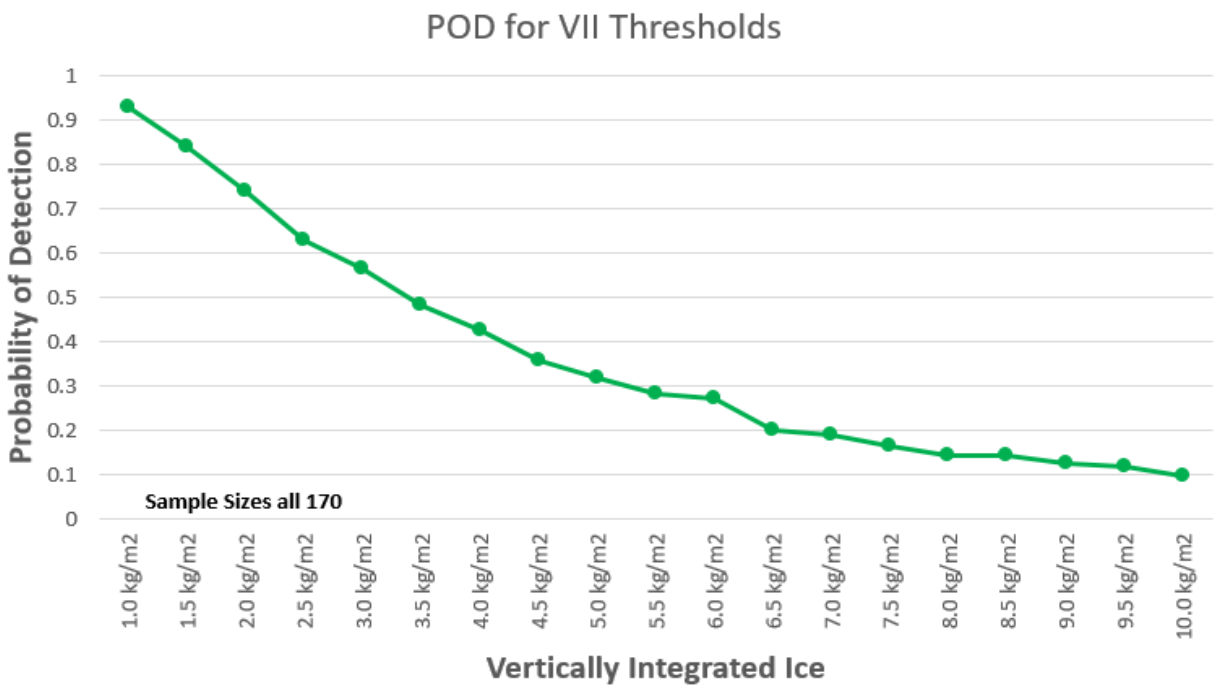

Figure 10. The POD for VII thresholds from 1 to 10 kg m^{-2}. The sample size for all thresholds is 170, which is the total number of cells that produced lightning.

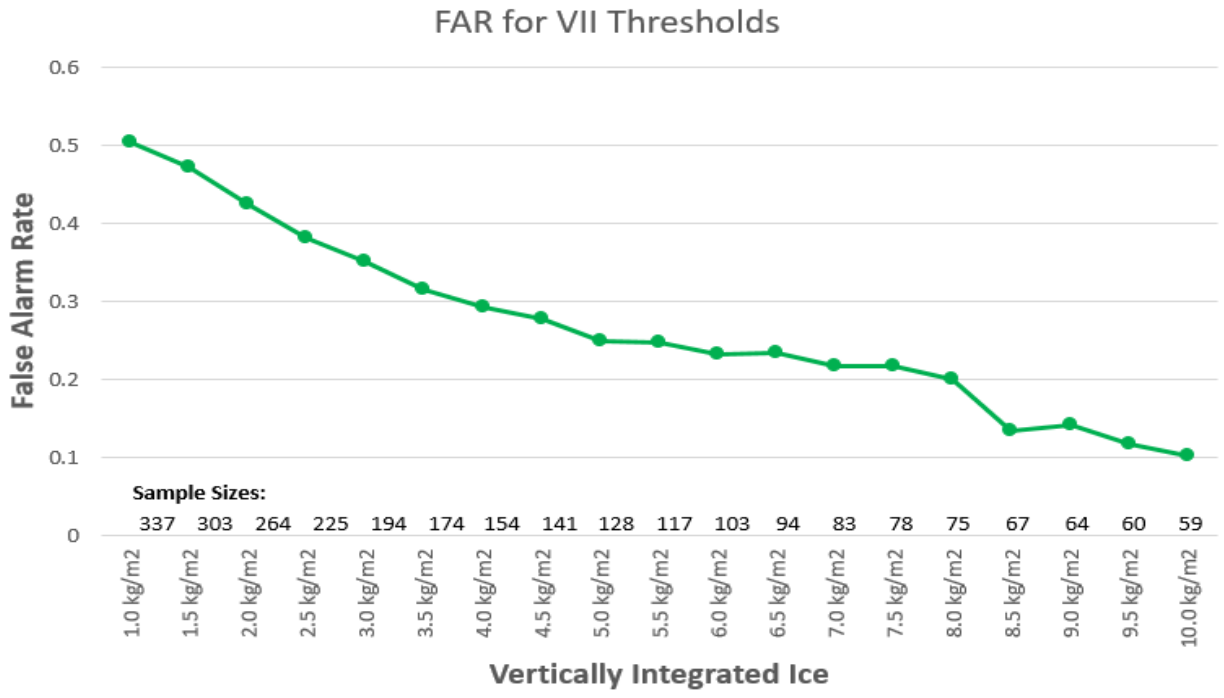

Figure 11. The FAR for VII thresholds from 1 to 10 kg m^{-2}. The sample size noted for each threshold is the total number of cells (whether correct, false alarm, missed event) observed at each threshold.

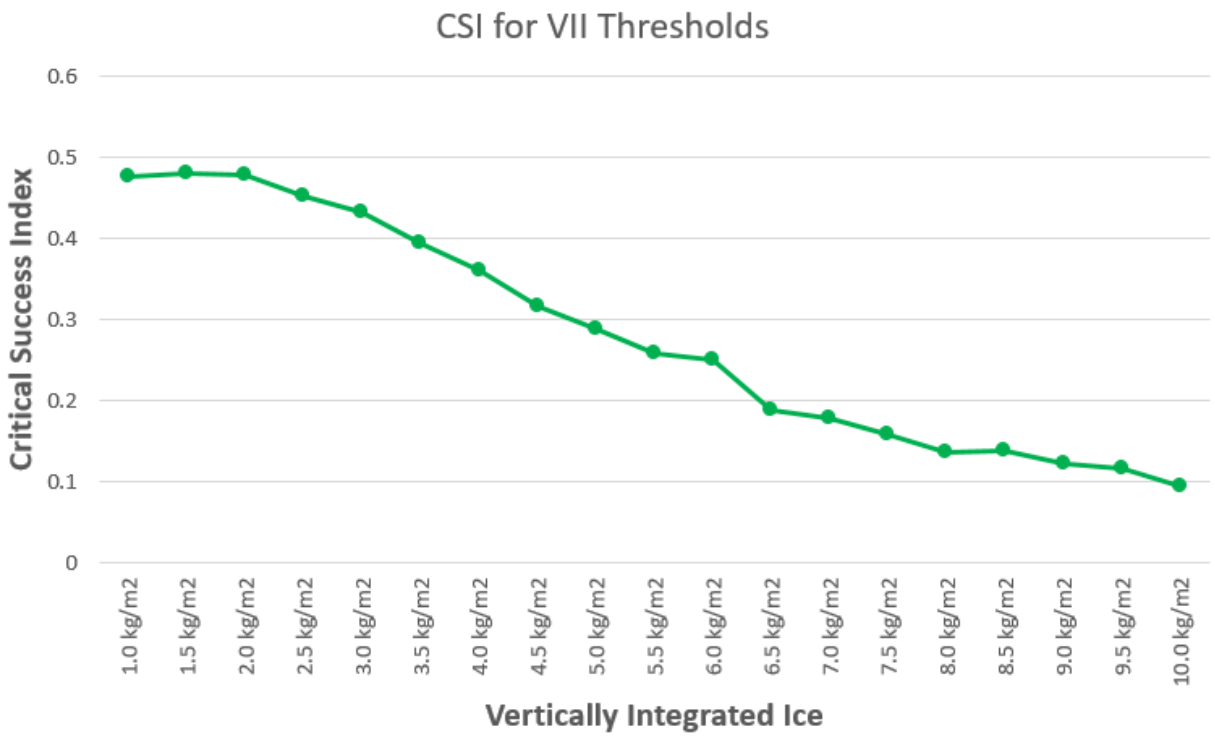

Figure 12. The CSI for VII thresholds from 1 to 10 kg m^{-2}.

Looking specifically at the best performing thresholds as determined by the highest CSI scores, interesting findings emerge. The best VII predictors, from 1.0 kg m^{-2} to 2.0 kg m^{-2}, had CSI values of 0.48, essentially identical to the best isothermal reflectivity predictors, which were 40 dBZ at -10°C and 30 dBZ at -20°C. These peak CSI values were generally lower than those found by Mosier et al. (2011) for similar thresholds, but comparable to those found by Seroka et al. (2012). Both POD and FAR were higher in this study than in Mosier et al. (2011), which could be due in part to differences in cell tracking, location, and/or time of year analyzed. The average lead time of the best VII predictors ranged from 19.2 minutes at 1.0 kg m^{-2} to 15.3 minutes at 2.0 kg m^{-2}. For isothermal reflectivity thresholds, the average lead time was 17.8 minutes for 30 dBZ at -20°C and 16.1 minutes for 40 dBZ at -10°C. These lead times were significantly more than was found by both Mosier et al. (2011) and Seroka et al. (2012). A significant portion of this advantage may be due to the subjective nature of this study, which allowed for a cell to be tracked before the STI algorithm placed an ID tag on it. The previous two studies did not begin computing statistics for a cell until it was formally identified by their tracking algorithm. Given the similar CSI scores, the slightly better lead times of the VII predictors should give forecasters confidence in using the relatively new MRMS VII product to predict CG initiation for DSS purposes.

4. Conclusions and Future Work

Previous research has shown the potential of forecasting CG lightning using radar reflectivity thresholds at various isothermal heights (Buechler and Goodman 1990; Gremillion and Orville 1999; Wolf 2007).

Research by Mosier et al. (2011) and Seroka et al. (2012) demonstrated the value of using VII as well, although these studies were done prior to VII being available to forecasters in real-time. The previous studies examined datasets in Texas and Florida, whereas this study is believed to be the first to examine VII in New England. This paper showed that VII can be a very useful nowcasting tool in northern climates as an indicator that a convective cell may have the potential to produce CG lightning. When using the VII as an indicator of potential for CG lightning the highest PODs (0.93) and FARs (0.50) were associated with the lowest value of VII, which at the time that the study was conducted was 1.0 kg m^{-2}. The greatest average lead time to first CG strike of 19.2 minutes was noted with the lowest VII threshold of 1.0 kg m^{-2}. The greatest average lead time using isothermal reflectivity of 25.3 minutes was observed along the -10°C isotherm at the 25 dBZ reflectivity threshold.

At the time of this study's data collection, the lower bound of VII values displayable on AWIPS was 1.0 kg m^{-2}, but this lowest displayable value has since been decreased to 0.5 kg m^{-2}. Given the finding in Mosier et al. (2011) that VII values over 0.42 kg m^{-2} represented a sufficient ice mass for cloud electrification, the authors suggest that using VII values less than 1.0 kg m^{-2} and possibly as low as 0.5 kg m^{-2} could provide added lead time in the detection of CG lightning. Values much below 0.5 kg m^{-2} may indicate an insufficient amount of ice mass for cloud electrification, and the incidence of CG would be very low. Based on previous research and our study it is likely that the FAR will further increase as VII values drop below 1.0 kg m^{-2} but that the CSI will still remain high enough to provide value for certain types of decision makers. When there are convective cells with a CG lightning threat, lower values of VII less than 1.0 kg m^{-2} would likely provide added lead time with high POD, which could still offer value for some users, despite the lower CSI and higher FAR.

The production of a graphical hazards map depicting categorical lightning risk is envisioned as a tool to assess the near term, i.e. less than 1 hour, risk of CG lightning for the public as well as for those tasked with providing for public safety. Currently the NWS produces an experimental enhanced Hazardous Weather Outlook that displays CG lightning risk level for days 1-7 which is based on forecasters' subjective confidence that lightning will occur. A rapid-updating tool that could be used by decision makers to express the CG risk on much shorter time scales using a combination of VII, radar reflectivity, and CG lightning data, and MRMS Cloud-to-Ground Lightning Density and Probability could prove valuable as a decision support resource, and possibly prevent injury or even death from CG lightning. An experimental product could be developed to test the utility of such a product. The product could fall under the umbrella of Forecasting a Continuum of Environmental Threats (FACETs) (Rothfusz et al. 2018), in which site specific weather hazard information that conveys grid based probabilities of CG lightning would be displayed. Calhoun et al. 2018 (Fig. 13) and Stano et al. 2019 describe some recent lightning hazard prototype efforts.

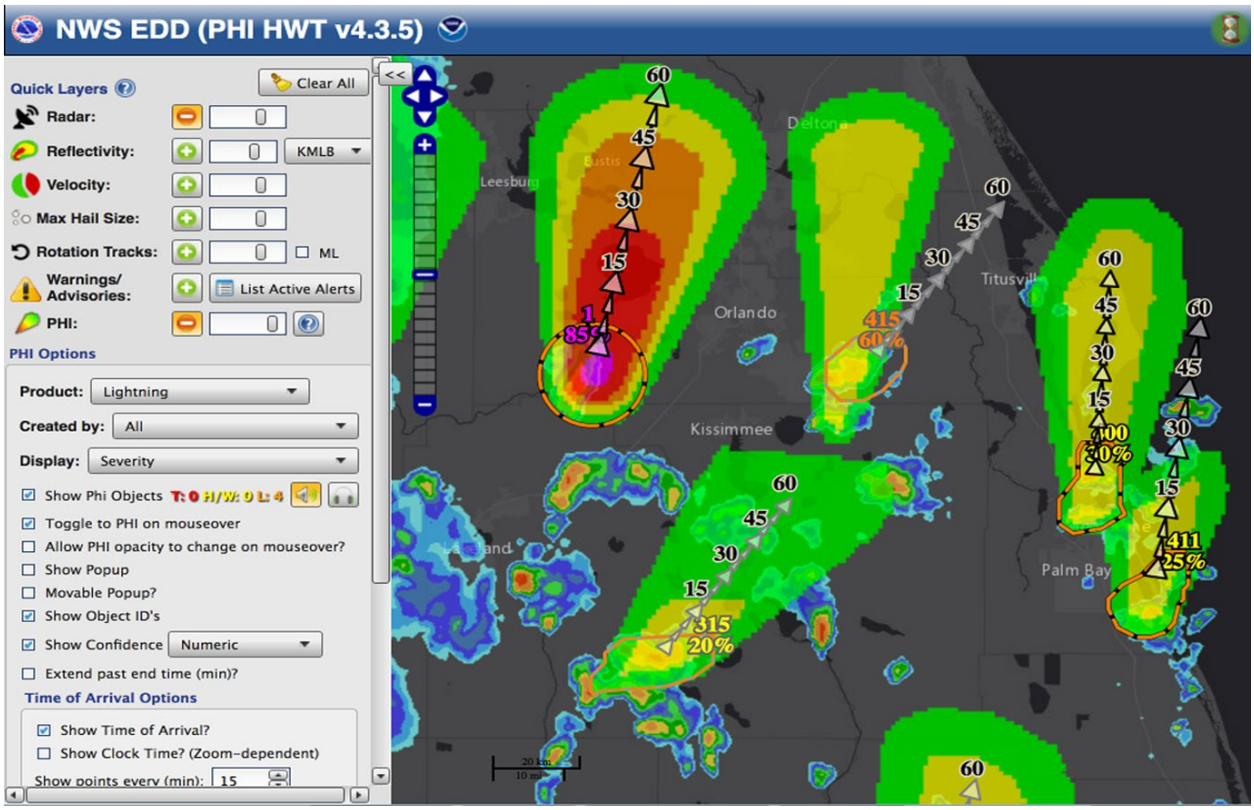

Figure 13. Experimental probabilistic cloud-to-ground lightning guidance evaluated during the 2017 Hazardous Weather Testbed Experiment. Current probabilities and forecasts (numeric for current probabilities, graphical for forecast), time of arrival (15 min intervals) along central track, and human (dark/orange/black) and automated (light orange) objects are shown over current reflectivity. From Calhoun et al. 2018.

Examining the use of VII as a tool for potential CG lighting detection in stratiform precipitation regimes may be a worthy endeavor. Furthermore, it would be valuable to objectively analyze a larger number of cells over multiple seasons, and perhaps over several years similar to the Mosier study, with an expansion across different regions or sub-regions of the U.S. to see if any regional, sub regional, or seasonal trends can be detected in the data. This would also provide climatological insights into the long term patterns of CG lightning. If such a study is conducted, it would be worth studying the VII values at both initiation and cessation of CG to see how they compare to the Seroka et al. (2012) and Mosier, et al. (2011) studies.

5. Acknowledgements

Thanks to Patrick Maloit (Meteorologist-in-Charge), Todd Foisy (Science and Operations Officer), and Gregory Cornwell (Forecaster) of the NWS forecast office in Caribou, Maine and Jeff Waldstreicher and Brian Miretzky (Scientific Services Division) of the NWS Eastern Region Headquarters for their thoughtful reviews and suggestions related to this publication. Don Britton (Meteorologist-in-Charge), Dave Bernhardt

(Science and Operations Officer), and Paul Nutter (Lead Forecaster) from the NWS forecast office in Great Falls, Montana, are also thanked for providing very helpful feedback. Thanks are extended to Matt Mosier of the Storm Prediction Center and Ted Ryan (Science and Operations Officer) of the NWS forecast office in Fort Worth, Texas, for their explanations of prior research and attempts to field VII operationally prior to MRMS.

6. References

Buechler, D.E., and S. J. Goodman, 1990: Echo size and asymmetry: Impact on NEXRAD storm identification. *J. Appl. Meteor.*, 29, 962-969, https://doi.org/10.1175/1520-0450%281990%29029%3C0962%3AESAAIO%3E2.0.CO%3B2

Calhoun, K. M., T. C. Meyer, K. Berry, H. Obermeier, S. J. Sanders, C. A. Shivers, C. D. Karstens, J. P. Wolfe, and K. E. Klockow, 2018: Cloud-to-Ground Lightning Probabilities and Warnings within an Integrated Warning Team. AMS Special Symposium on Impact-Based Decision Support Services, Austin, TX, https://ams.confex.com/ams/98Annual/webprogram/Paper329888.html

Carey, L. D. and S.A. Rutledge, 2000: The relationship between precipitation and lightning in tropical island convection: A C-band polarimetric study. *Mon. Wea. Rev,* 128, 2687-2710 https://doi.org/10.1175/1520-0493(2000)128%3C2687:TRBPAL%3E2.0.CO;2

Gremillion, M.S., and R.E. Orville, 1999: Thunderstorm characteristics of cloud-to-ground lightning at the Kennedy Space Center, Florida: A study of lightning initiation signatures as indicated by the WSR-88D. *Wea. Forecasting*, 14, 640-649, https://doi.org/10.1175/1520-0434(1999)014%3C0640:TCOCTG%3E2.0.CO;2

Holle, R. L., 2018. Lightning Deaths by State and Deaths Population Weighted, NOAA Lightning Safety Web Site. [Available online at https://www.weather.gov/media/safety/08-17Fatality_Map_state.pdf]

Holle, R. L., and Coauthors, 1992: Cloud-to-ground lightning related to deaths, injuries, and property damage in central Florida. Proc. Int. Conf. on Lightning and Static Electricity, Atlantic City, NJ, FAA Rep. DOT/FAA/CT-92/20, 66-1–66-11.

Jensenius J.S., Jr, 2019. A Detailed Analysis of Lightning Deaths in the United States from 2006 through 2018. [Available online at https://www.weather.gov/media/safety/Analysis06-18.pdf]

Johnson, J.T., and Coauthors, 1998: The Storm Cell Identification and Tracking Algorithm: An Enhanced WSR-88D Algorithm. Wea. Forecasting, 13, 263-276, https://doi.org/10.1175/1520-0434(1998)013%3C0263:TSCIAT%3E2.0.CO;2

Mosier, R.M., and Coauthors, 2011. Radar Nowcasting of Cloud-to-Ground Lightning over Houston, Texas. Wea. Forecasting, **26**, 199-212 Corrigendum 586-590, https://doi.org/10.1175/2010WAF2222431.1

Rothfusz, L.P., R. Schneider, D. Novak, K. Klockow-McClain, A.E. Gerard, C. Karstens, G.J. Stumpf, and T.M. Smith, 2018: FACETs: A Proposed Next-Generation Paradigm for High-Impact

Weather Forecasting. *Bull. Amer. Meteor. Soc.,* **99**, 2025-2043. https://doi.org/10.1175/BAMS-D-16-0100.1

Seroka, G.N., and Coauthors, 2012. Radar Nowcasting of Total Lightning over the Kennedy Space Center. Wea. Forecasting, **27**, 189-204, https://doi.org/10.1175/WAF-D-11-00035.1

Smith, T.M., and Coauthors, 2016. Multi-Radar Multi-Sensor (MRMS) Severe Weather and Aviation Products. *Bull. Amer. Meteor. Soc.*, **97**, 1617-1630, https://doi.org/10.1175/BAMS-D-14-00173.1

Stano, G. T., M. R. Smith, and C. J. Schultz, 2019: Development and evaluation of the GLM stoplight product for lightning safety. J. Operational Meteor., 7 (7), 92-104, https://doi.org/10.15191/nwajom.2019.0707

Wolf, P., 2007: Anticipating the initiation, cessation, and frequency of cloud-to-ground lightning, utilizing WSR-88D reflectivity data. NWA Electron. J. Oper. Meteor., 8 (1), 1-19. [Available online at http://nwafiles.nwas.org/ej/pdf/2007-EJ1.pdf]